Atmospheric Environment 43 (2009) 3941–3950

Contents lists available at ScienceDirect

Atmospheric Environment

journal homepage: www.elsevier.com/locate/atmosenv

Apportioning black carbon to sources using highly time-resolved ambient measurements of organic molecular markers in Pittsburgh

Andrew T. Lambe [a], Jennifer M. Logue [a], Nathan M. Kreisberg [b], Susanne V. Hering [b], David R. Worton [c], Allen H. Goldstein [c], Neil M. Donahue [a], Allen L. Robinson [a,*]

[a] Center for Atmospheric Particle Studies, Carnegie Mellon University, USA
[b] Aerosol Dynamics Inc, USA
[c] Department of Environmental Science, Policy and Management, University of California – Berkeley, USA

ARTICLE INFO

Article history:
Received 10 January 2009
Received in revised form
6 April 2009
Accepted 7 April 2009

Keywords:
Organic aerosols
Black carbon
Molecular markers
Thermal desorption aerosol GC/MS (TAG)
Source apportionment
PMF
CMB

ABSTRACT

We present highly time-resolved measurements of organic molecular markers in downtown Pittsburgh, which are used to investigate sources contributing to atmospheric aerosols in the area. Two-hour average concentrations of condensed-phase and semivolatile organic species were measured using a Thermal Desorption Aerosol GC/MS (TAG). Concentrations for mobile source markers like hopanes had regular diurnal and day-of-week patterns. Pairing high time-resolved measurements with meteorological data helped identify contributions from known point sources for markers correlated with wind direction. Black carbon (BC), volatile organic compounds (VOCs) and organic molecular markers were apportioned to sources using the Chemical Mass Balance (CMB) and Positive Matrix Factorization (PMF) receptor models. Diesel and gasoline mobile source factors were identified as the main sources of BC in the downtown Pittsburgh area, contributing 67% and 20% of the study-average BC. 13% of the BC was associated with a source factor tentatively identified as an industrial or regional source. The high time resolution of the TAG has the potential to provide important new insight into source apportionment efforts using organic molecular marker measurements.

1. Introduction

Significant advances in instrumentation capable of measuring atmospheric aerosols have been made over the last decade (Solomon and Sioutas, 2008; Wexler and Johnston, 2008). These instruments have provided higher total mass recovery, more detailed chemical speciation (e.g. $PM_{2.5}$ ions, carbon fractions, organic molecules), and better time resolution, providing new insight into the complexity of aerosols. Detailed chemical speciation data are critical for source apportionment – particularly for organic aerosols, where multiple contributing sources potentially confound interpretation of bulk organic carbon (OC) data. OC sources include vehicles, biomass burning, cooking, industrial activity, and secondary organic aerosol (SOA) formation. High time resolution also greatly aids source apportionment by capturing dynamic processes related to source activity, such as rush hour traffic from mobile sources and emissions plumes from point sources. The ideal instrument would combine detailed chemical speciation with high mass recovery and time resolution.

Source apportionment of OC has traditionally relied on manual collection of integrated 12- or 24-h quartz filter/polyurethane foam (PUF) plug samples followed by offline gas chromatography with mass spectrometry (GC/MS) analysis. This method allows quantitation of source-specific organic marker compounds at the molecular level, which have been used to apportion sources of atmospheric aerosols in many areas of the country (Schauer et al., 1996; Zheng et al., 2002; Ondov et al., 2006; Robinson et al., 2006c; Shrivastava et al., 2007; Jaekels et al., 2007). The method requires large samples, which sacrifices time resolution. Sample collection and extraction from filter media is also extremely time- and labor-intensive, which limits the number of samples and frequency of measurements.

Recently, a novel *in situ* Thermal Desorption Aerosol GC/MS (TAG) was developed by researchers at the University of California – Berkeley and Aerosol Dynamics Inc. (Williams et al., 2006, 2007; Goldstein et al., 2008b). This instrument is an automated adaptation of direct sample introduction TD-GC/MS and semi-continuous inorganic aerosol methods (Stolzenburg and Hering, 2000; Falkovich and Rudich, 2001; Waterman et al., 2001; Ho et al., 2008). While the TAG's mass recovery at the molecular level is low (like filter-based techniques), the high time resolution is a significant advantage over longer integrated samples. Molecular-level speciation also

* Corresponding author.
E-mail address: alr@andrew.cmu.edu (A.L. Robinson).

1352-2310/$ – see front matter © 2009 Elsevier Ltd. All rights reserved.
doi:10.1016/j.atmosenv.2009.04.057

complements other high time-resolved techniques such as the Aerodyne AMS (Jayne et al., 2000). The TAG has been deployed in field campaigns where it has been used to interpret concurrent bulk measurements from other instruments (Williams et al., 2007; Goldstein et al., 2008b). This method can provide around-the-clock speciation of organic aerosols at high time resolution, but it requires continued deployment and evaluation. This paper describes an application of the TAG to characterize organic aerosol composition in downtown Pittsburgh. The high time-resolved data are used to characterize diurnal patterns of molecular marker concentrations. The data are also analyzed using both the chemical mass balance (CMB) and positive matrix factorization (PMF) models to apportion black carbon (BC) to sources and estimate gasoline-diesel split contributions in Pittsburgh.

2. Methods

2.1. Field site

The TAG and other instruments were deployed in downtown Pittsburgh from February to May 2008. Measurements were taken out the window of a 4th floor office suite in the Diamond Building, located at the intersection of Fifth Ave and Liberty Ave. The site is less than a mile from three major highways (I-279, I-579, and I-376), and is close to many city bus routes. Other instrumentation deployed at the site included an automated VOC-GC/MS system (Logue et al., submitted for publication) that provided hourly measurements of a suite of volatile organic compounds (VOCs), and a multi-wavelength Aethalometer (Magee Scientific, Hansen et al., 1984) that measured BC. Hourly wind-direction data were measured at a monitoring station about 3 miles southeast of the field site.

2.2. TAG measurements

The TAG instrument and operating principles have been described in detail elsewhere (Williams et al., 2006, 2007). Briefly, TAG has two modes of operation: (1) ambient sampling with concurrent GC/MS analysis of the previous sample, and (2) thermal desorption of a sample onto the GC column. During sampling, ambient air was pulled through a $PM_{2.5}$ cyclone into a custom collection inlet fabricated by Aerosol Dynamics, Inc. (Berkeley, CA). The inlet humidifies the particles at an RH of 75–95% to increase adhesion and minimize bounce in the collection cell. This cell was maintained at 30 °C during collection. Following sample collection, the cell was isolated from the sample line and heated to 50 °C to purge water and volatile compounds with 50 sccm helium carrier gas. The cell was then ramped from 50 °C to 300 °C at approximately 25 °C min^{-1} and held for 3 min, after which a 6-port valve switched the cell to the inject position. Helium carrier gas then flowed through the cell, transfer lines and a 6-port valve at 1 sccm to transfer the sample to the GC column (maintained at 45 °C). The purging/desorption sequence is adjustable. During desorption all transfer lines were maintained at 300 °C to minimize losses. The valve rotor and transfer lines in the sample transfer path were chemically passivated using an Inertium coating (AMCX; Bellefonte, PA).

Online GC/MS analysis was performed using an Agilent 5890 GC coupled to an Agilent 5971 MSD. Chromatographic separation was achieved using a Restek Rtx-5MS fused capillary column (30 m × 0.25 mm × 0.25 μm) with 1 mL min^{-1} flow in helium. The GC method took 1 h to complete and used the following temperature protocol: initial temperature 80 °C, ramp 50 °C min^{-1} to 45 °C, hold for injection of thermally desorbed sample; ramp 8.6 °C min^{-1} to 310 °C, hold 10 min; ramp 70 °C min^{-1} to 80 °C final temperature for the start of the next run. The MSD was operated in Selected Ion Monitoring (SIM) mode to improve measurement signal-to-noise. Tables 5 and 6 in Supporting Information show the SIM method used for sample analysis.

Two sampling protocols were employed during the campaign. The first involved sampling on a 26-h cycle for about three weeks. This cycle produced twelve 90-min samples and two blank samples every 26 h. A calibration standard, described in more detail in the next section, was normally injected during one of the blank samples. This sampling procedure allowed for maximum resolution of 2 h, including 30 min thermal desorption time after each 90-min sample collected for a suite of organic molecular markers. In this mode, 286 ambient, 24 calibration, and 28 blank samples were collected from 2/26/08 to 4/4/08. Samples were not blank-corrected because blank levels were minor (<10%) for all markers used for source apportionment. Measurements were not taken from 3/4/08 to 3/15/08 because of power issues at the site. Because of these power issues and shorter offline periods for routine maintenance, the TAG was online about 67% of the time during this period.

The second protocol sampled on a 24-h cycle. This cycle used three 4-h daytime samples (6:30 AM–10:00 AM, 11:30 AM–3:00 PM, 3:00 PM–7:00 PM), one 10-h overnight sample (8:30 PM–6:30 AM), and 2 blank samples following the morning and evening daytime samples. The calibration standard was normally injected during one of the blank samples. In this mode, 147 ambient, 29 calibration, and 43 blank samples were collected from 4/19/08 to 5/27/08. Including a brief power outage and offline periods for routine maintenance, the TAG was online about 95% of the time during this period. This protocol provided more data above detection limit at night and on weekends when concentrations were often below the instrument detection limit with shorter 90-min samples.

2.3. TAG calibration

The TAG was calibrated using a liquid standard that was manually injected directly into the collection cell in a similar manner as has been described previously (Williams et al., 2007; Kreisberg et al., 2009). The standard was prepared by combining stock solutions of *n*-alkanes and PAHs (Accustandard DRH-008S-R1 and H-QME-01; Chemservice 1007S, 1052S, 1047S), hopanes (Chiron 0615,27; 1321,29; 0613,30; 1339,31), cholesterol and β-sitosterol (Sigma–Aldrich), and custom-prepared solutions of the remaining compounds in the standard (Sigma–Aldrich). Information about analytical precision and limits of quantitation (LOQ) for individual analytes in the standard is presented in Tables 1–4 in Supporting Information. A multipoint calibration was performed at the beginning of each measurement period after autotuning the MSD. Because sensitivity of the MSD decayed over time, a single-point calibration was performed on subsequent measurement days (Kreisberg et al., 2009). A multipoint calibration was also performed at the end of the second major measurement campaign from 4/19/08 to 5/27/08.

This calibration procedure does not account for sample collection efficiency (CE), which may be less than 100% for semivolatile analytes and for ultrafine particles below the impactor cutpoint. In previous work, the TAG CE for particles with D_p = 100 nm was about 65% for potassium chloride (solid) and 85% for oleic acid (liquid) at a cell RH = 60–70%, and dropped off significantly for smaller diameters (Williams et al., 2006). For light-duty vehicles, ≤20–25% of the mass of hopanes and PAHs is contained in ultrafine particles with $D_p \leq 100$ nm (Riddle et al., 2007). For heavy-duty vehicles, as much as 50% of the mass of hopanes is contained in ultrafine particles, but in most cases less than 30% of the mass of hopanes and PAHs are in the ultrafine size range. However, these

values are for fresh emissions; particles emitted by motor vehicles will grow in the atmosphere due to condensation and coagulation, which will improve collection efficiencies during ambient studies. We assumed a CE of 100% for all measurements presented here, and this assumption should be within a factor of 2 of the true CE for condensed-phase marker compounds. The TAG CE for vapors has not been characterized. Given that the method is designed to minimize adsorption of gas-phase artifacts, CE is significantly lower for vapors than for particles.

2.4. Source apportionment

The molecular marker dataset was analyzed using the chemical mass balance (CMB) and positive matrix factorization (PMF) models to investigate sources of BC in the downtown Pittsburgh area. These models solve the equation

$$x_{ij} = \sum_{k=1}^{p} g_{ik} f_{kj} + e_{ij} \quad (1)$$

An ambient data matrix x_{ij} (concentrations of species j in sample i) is input into the model, and the objective is to minimize the residual error e_{ij} between x_{ij} and a set of p reconstructed source factors (Friedlander, 1973; Paatero and Tapper, 1994). g_{ik} is the contribution of factor k to sample i, and f_{kj} is the contribution to species j from factor k in that sample. Equation (1) was solved with EPA PMF 3.0 software (Norris et al., 2008), which uses the multilinear engine (ME-2; Paatero, 1999). PMF minimizes the residual error and solves for g_{ik} and f_{kj} by minimizing the objective function Q:

$$Q = \sum_{i=1}^{n} \sum_{j=1}^{m} \left(\frac{e_{ij}}{u_{ij}} \right) \quad (2)$$

where u_{ij} is the measurement uncertainty of species j in sample i.

Compounds included in the PMF and CMB models were chosen based on low measurement uncertainties ($\leq$20%), high signal-to-noise, or detection in sources profiles reporting BC emissions (Lavrich and Hays, 2007; Ho et al., 2008). Fractional errors for fitting species are presented in Table 7 in Supporting Information and were based on calibration data for TAG and VOC-GC/MS compounds presented in Tables 1–4 (Supporting Information). Uncertainty in BC measurements was calculated at 5% based on the standard deviation of measurements across seven aethalometer wavelengths averaged over 90 min. The LOQ for BC measurements was estimated to be 0.1 μg m^{-3}. Chemical mass balance (CMB) analysis was performed with the EPA CMB8.2 software (Coulter, 2004) and the results were compared to PMF factors. BC and hopanes/steranes (Table 3 in Supporting Information plus 17a(H),21b(H)-hopane and 22S-17a(H),21b(H)-30-homohopane, minus 17b(H),21b(H)-hopane) were used as CMB fitting species. Composite source profiles from Fujita et al. (2007a) were used as inputs to the CMB model.

3. Results and discussion

3.1. Temporal and wind-direction patterns of select molecular markers

Fig. 1 shows time series of selected molecular markers to illustrate the distinctive temporal patterns of ambient concentrations. These patterns reflect the influence of different sources, activity patterns, and changing meteorology on molecular marker concentrations. Fig. 1a shows the time series for norhopane and hopane measured over a three-week period. Hopanes are associated with fossil-fuel combustion and are frequently used as molecular markers for mobile sources (Rogge et al., 1993a). The temporal profile suggests some sort of diurnal pattern arising from changes in motor vehicle activity. Hopanes were among the most dynamic molecular markers measured – concentrations varied by more than a factor of 20. High concentrations were routinely observed in the morning, with very high concentrations (up to 4 ng m^{-3}) observed on certain days. At night hopane levels were much lower and often below detection limits. The large variability indicates the strong influence of local sources. Levels are highest in the morning during rush hour and then decrease due to vertical mixing.

As shown in Figs. 2 and 3, norhopane showed strong average diurnal and day-of-week patterns characteristic of mobile source emissions. Daily maximum levels occurred in the morning, coincident with rush hour traffic and low mixing height, and generally consistent with near-roadway measurements of diurnal patterns in other urban locations (Thoma et al., 2008). Concentrations decreased throughout the day due to increased vertical mixing. Interestingly, there was not a late afternoon spike in norhopane concentrations, presumably because the evening rush hour emissions were offset by a higher mixing layer. Photochemical oxidation of norhopane could also be contributing to observed diurnal patterns (Robinson et al., 2006a; Weitkamp et al., 2008). Norhopane levels were lowest in the evenings, before increasing overnight due to a suppressed mixing layer. Fig. 3 indicates that norhopane levels were significantly higher on weekdays (0.39–0.57 ng m^{-3}) than on weekends (0.21–0.28 ng m^{-3}). These differences were statistically significant ($p < 7.4 \times 10^{-9}$, Student's independent two-tailed t-test). Weekday differences were generally not statistically significant, though Wednesday levels were higher than Mondays ($p < 0.016$) and Thursdays ($p < 0.046$) with 95% confidence. Other hopanes exhibited patterns similar to norhopane. Fig. 4b also shows elevated norhopane and BC concentrations when wind arrives from the south/southeast. Major point sources are located to the northwest (Neville Island) and south–southeast of downtown Pittsburgh, and there are major highways on three sides of the site. n-Alkanes (Fig. 1b) had a similar temporal profile as the hopanes, and most of the n-alkanes (C13–C27) were also well correlated with BC. Larger n-alkanes ($\geq$C28) were often below detection limits, but occasional large spikes during plume events were observed. Levels during the event shown in Fig. 1e were disproportionately high relative to the other n-alkanes.

Fig. 1c shows the time series for 9-fluorenone and 9,10-anthracenedione. These compounds have been detected in emissions from mobile sources, natural gas home appliances, and industrial-scale boilers (Rogge et al., 1993a,b, 1997); they have also been proposed as markers for secondary sources through oxidation of parent PAHs (Goldstein et al., 2008a). 9-Fluorenone and 9,10-anthracenedione were characterized by generally low and stable concentrations punctuated by occasional spikes. These spikes suggest local point source emissions contributing to regional background concentrations. Figs. 2 and 3 indicate that 9-fluorenone exhibited no diurnal and day-of-week patterns. Average levels were somewhat higher on weekdays (2.0–3.3 ng m^{-3}) than weekends (1.7–1.9 ng m^{-3}), and these differences were statistically significant ($p < 1.1 \times 10^{-4}$). Differences between Tuesday measurements and other weekdays were also statistically significant at 95% confidence levels ($p < 0.044$, $p < 0.0043$, $p < 0.042$) for Mondays, Thursdays, and Fridays.

Phthalic acid has been proposed as a marker for secondary organic aerosols (Schauer et al., 1996; Rogge et al., 1996), and Cass, and had a very different temporal profile than the primary vehicle markers. Average diurnal and weekly trends are shown in Figs. 2 and 3. It remained relatively constant throughout the campaign and

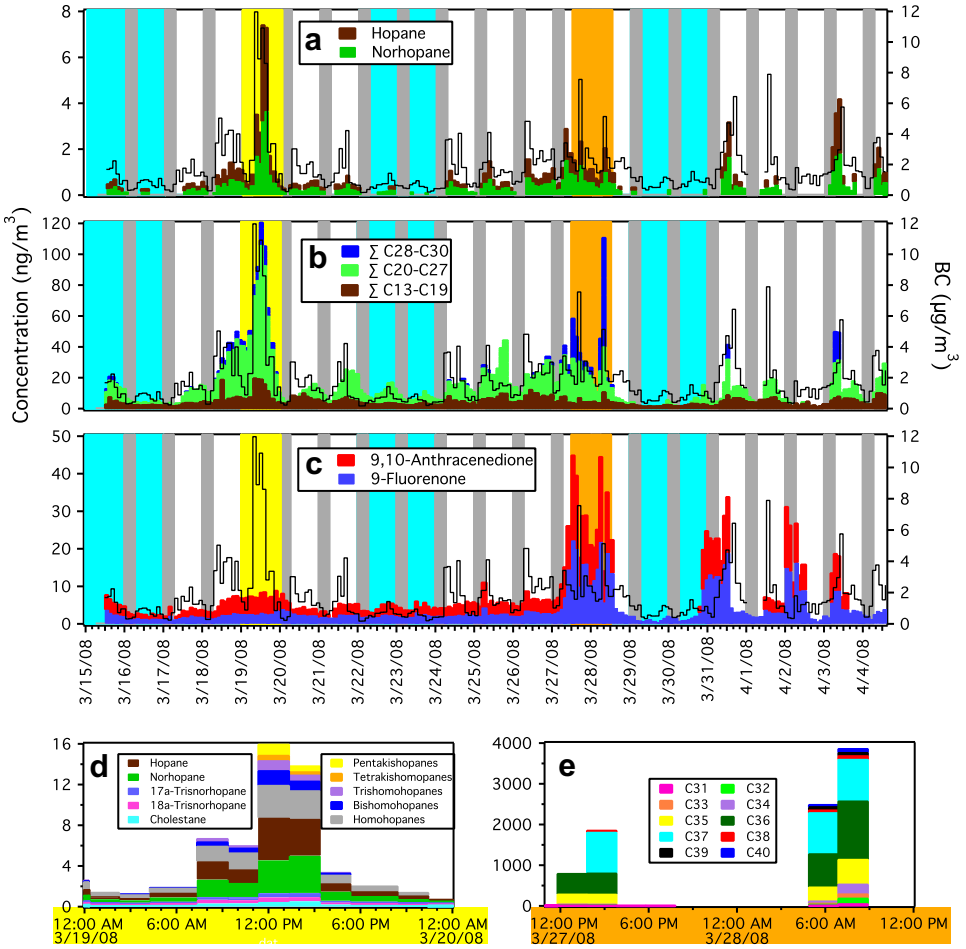

Fig. 1. Time series of selected marker compounds. Concentrations (left *y*-axes) are in ng m^{-3}. Grey bars are overnight periods (12–6 AM); cyan bars are weekends; black trace is BC concentration (µg m^{-3}) averaged over TAG sampling periods. Time series traces are stacked. (a) Norhopane and hopane, (b) *n*-alkanes, and (c) 9-fluorenone and 9,10-anthracenedione levels. Panels (d) and (e) show specific 24-h periods with high concentration events captured by TAG. (For interpretation of color in the figure legend, the reader is referred to the web version of the article.)

was poorly correlated with BC, suggesting a well-mixed regional source. There were no statistically significant differences between all weekday and weekend phthalic acid measurements. However, phthalic acid did have a clear diurnal pattern: levels build throughout the day which is consistent with formation from photooxidation of precursor species. Previous field work found phthalic acid strongly correlated with the Aerodyne AMS $m/z = 44$ signal as a marker for oxygenated organic aerosol (OOA), which builds up quickly in the daytime during periods of high photochemical activity (Takegawa et al., 2007).

Fig. 1d shows a high concentration event where many compounds reached their maximum levels measured during the

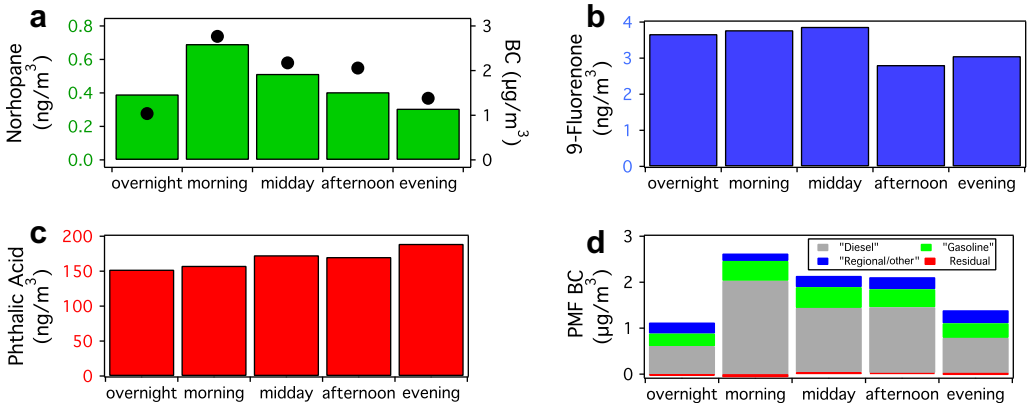

Fig. 2. (a)–(c) Average diurnal patterns for norhopane, BC (black dots), 9-fluorenone, and phthalic acid during overnight (12–6 AM), morning rush hour (6–11 AM), midday (11 AM–3 PM), afternoon/evening rush hour (3–8 PM), and evening (8 PM–12 AM) periods. Norhopane and BC reach daily maximum levels during morning rush hour. 9-Fluorenone did not have a diurnal pattern. Phthalic acid levels increase throughout the day from photooxidation of SOA precursors. (d) Average diurnal patterns for BC apportioned to PMF factors.

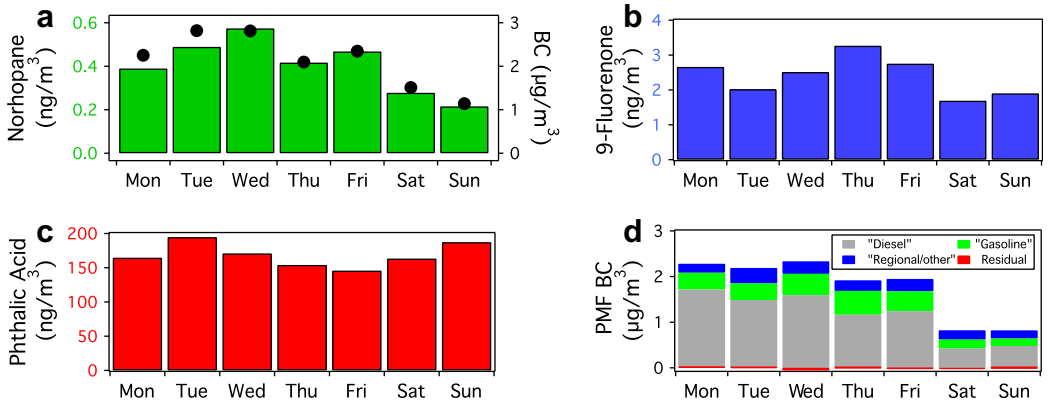

Fig. 3. (a)–(c) Average day-of-week trends for norhopane, BC (black dots), 9-fluorenone, and phthalic acid. Norhopane and BC show pronounced weekday–weekend trends, and 9-fluorenone shows weak weekday–weekend trends. Phthalic acid displays no day-of-week trends, consistent with regional/secondary sources. (d) Average day-of-week trends for BC apportioned to PMF factors.

study. Concentrations peaked during the middle of the day. This event occurred when the wind was from 218° and is represented on a wind rose plot in Fig. 4b and d. There are no known major sources in that direction; therefore, this event appears related to some specific meteorological conditions. However, we cannot rule out activity from an unknown source either.

Some compounds exhibited strong wind-directional dependence. For example, Fig. 4d indicates that tris(1,3-dichloro-2-propyl) phosphate (TDPP) and diethylhexyl phthalate (DEHP) concentrations were elevated when wind arrives from the south/southeast. These compounds are used as plasticizers and may be associated with industrial activity. TDPP is also used as a flame retardant in flexible and rigid polyurethane foams (Gold et al., 1978), and DEHP has been proposed as a marker for refuse burning (Simoneit et al., 2005).

Fig. 1e shows another event culminating in detection of extremely high levels of a suite of C30–C40 *n*-alkanes normally below detection limits. There is likely substantial uncertainty in quantitation of these compounds, but this does not affect interpretation of temporal patterns (the precision is excellent). PAHs often below detection limits (benzofluoranthenes, benzopyrenes, indeno(123cd)pyrene, benzo(ghi)perylene, and coronene) were also observed during this event, as shown in Fig. 1c and in Fig. 4c when the wind was from the east and northwest. Previous work has identified coke production as the major source of these PAHs in Pittsburgh (Robinson et al., 2006c). The spike correlated with wind

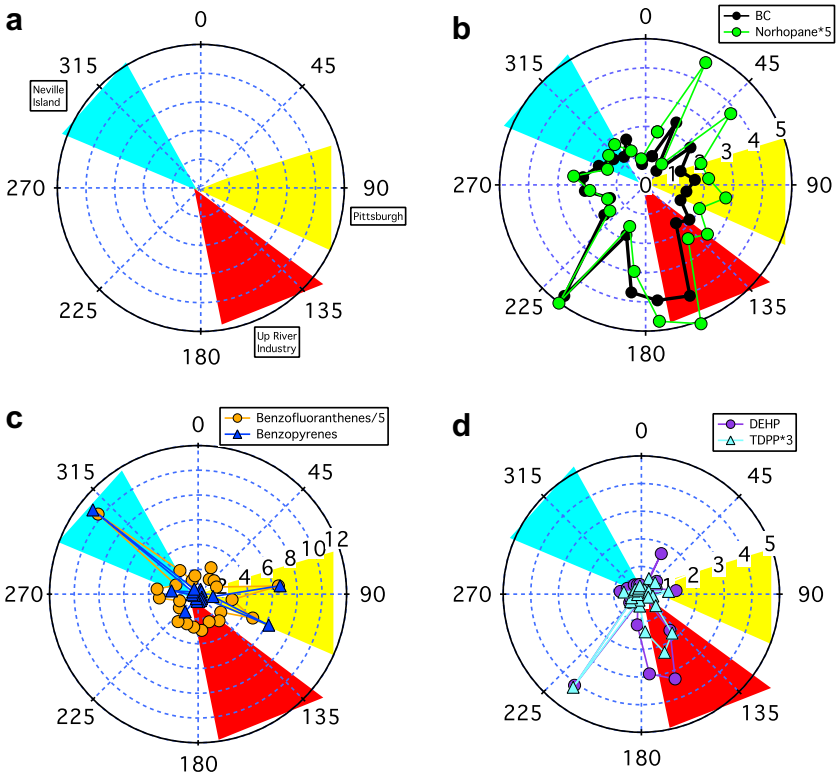

Fig. 4. Wind rose plots for molecular markers correlated with wind direction. Concentration data (ng m^{-3}, unless noted) was averaged into 15° bins. (a) Known source activity relative to downtown Pittsburgh location. (b) BC (μg m^{-3}) and norhopane. (c) Benzo(a + e)pyrenes and benzo(b + j + k)fluoranthenes. (d) Diethylhexyl phthalate (DEHP) and tris(1,3-dichloro-2-propyl) phosphate (TDPP) (raw counts $m^{-3} \times 10^{-6}$).

arriving from the northwest may reflect activity from coke production facilities on Neville Island.

3.2. Source apportionment of molecular markers and BC

PMF and CMB analyses were performed to investigate sources of molecular markers and BC. The compounds included in the PMF model are shown in Fig. 5a – many have been used previously in receptor models. Hopanes are associated with unburned lubricating oil and are frequently used as molecular markers for mobile source emissions. Alkanes and PAHs are associated with many anthropogenic sources that also emit BC and 6,10,14-trimethyl-2-pentadecanone may be a marker for secondary organic aerosol from vehicle exhaust (Shrivastava et al., 2007). We also included several anthropogenic VOCs (light aromatics and heptane) in the PMF model, in order to better separate the contributions of gasoline and diesel vehicles. Gasoline vehicle emissions are significantly enriched in these VOCs relative to diesel vehicles on a VOC:BC emissions basis measured in source tests (Schauer et al., 1999, 2002b) and tunnel studies (Schmid et al., 2001; Legreid et al., 2007). In addition, these VOCs have been apportioned almost exclusively to whole gasoline and gasoline vehicle emissions by previous receptor modeling studies (Schauer and Cass, 2000; Schauer et al., 2002a).

A key assumption in receptor models is that sources are fully represented by fitting species and source profiles. Nonpolar molecular markers used in this work are only a subset of those commonly used in CMB and PMF analysis for apportionment of OC and $PM_{2.5}$ (Zheng et al., 2002; Shrivastava et al., 2007). The ability to measure polar markers with TAG is limited, so sources like meat cooking and SOA are not considered in this analysis. Markers in Fig. 5a should be sufficient for apportionment of emissions from fossil-fuel combustion (such as motor vehicles and industrial sources), which in turn should be the dominant sources of BC. Wood smoke is a potentially important source of BC that is not well represented in our model. Shrivastava et al. (2007) apportioned 15% of the study-average BC in Pittsburgh to open burn and hardwood combustion factors, and Robinson et al. (2006b) apportioned 10% and 2% of OC to biomass smoke in the winter and spring, respectively, suggesting minor BC contributions. Based on previous work, we cannot rule out the possibility of about 10% of the study-average BC coming from wood combustion.

PMF analysis was performed on 275 samples collected from February to April 2008. A 3-factor solution was judged most interpretable; factor profiles for this solution are shown in Fig. 5. The 3-factor solution discussed here was obtained with a small negative rotation (FPEAK = −0.2) (Paatero et al., 2005), resulting in a *Q*-value of 3737 compared to the theoretical value of 8695. To help interpret the PMF solution, we compared the PMF factor profiles with literature source profiles measured during source tests. This was done using ratio–ratio plots, which are scatter plots of concentrations of two marker compounds normalized by a reference compound. The methodology is described in detail elsewhere (Robinson et al., 2006a,c). Some of the source profiles report elemental carbon (EC) rather than BC – this should not significantly affect interpretation of our results, as several studies report good agreement between BC and EC in urban areas (Allen et al., 1999; Babich et al., 2000; Park et al., 2002).

Fig. 6a shows a ratio–ratio plot of norhopane and hopane normalized by BC. The published source profiles (Schauer et al., 1999, 2002b; Fujita et al., 2007a,b) and the PMF factor profiles are represented by individual points. The ambient data organize along a diagonal line that is bracketed by the source and factor profiles. This means that hopane and EC data can be described by linear mixing of appropriate combinations of source profiles. The PMF factors also bracket most of the data. A few points lie outside the

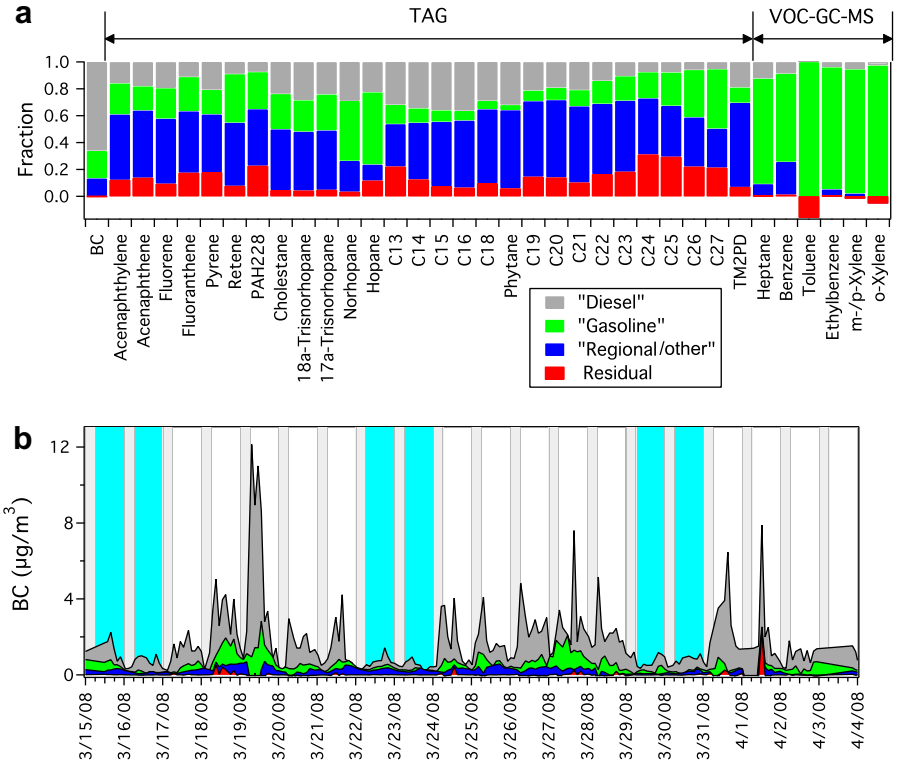

Fig. 5. (a) 3-Factor PMF apportionment (FPEAK = −0.2; PAH228 = benz(*a*)anthracene + chrysene; TM2PD = 6,10,14-trimethyl-2-pentadecanone). One factor explained 67% of BC ("diesel"). Another explained 20% of BC ("gasoline"). Remaining 13% BC associated with a "regional/other" source. (b) Time series for BC apportioned to each source factor; grey bars are overnight periods (12–6 AM) and cyan bars are weekends. (For interpretation of color in the figure legend, the reader is referred to the web version of the article.)

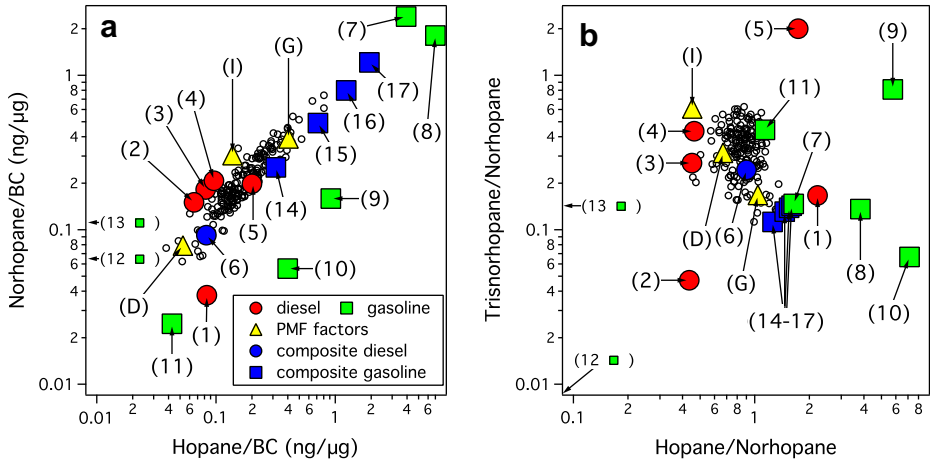

Fig. 6. Ratio–ratio plots of hopanes and BC. Ambient data shown in black circles and data representing source profiles (Schauer et al., 1999; Fujita et al., 2007a,b) shown in colored markers: (1) Fujita MDD, (2) Fujita HW, (3) Fujita HDD, (4) Fujita HCS, (5) Schauer MDD, (6) Fujita MDD-HDD (50–50) composite, (7) Fujita SI-HC, (8) Fujita SI-HW, (9) Fujita SI-BW, (10) Fujita SI-BC, (11) Schauer catalyst auto, (12) Fujita SI-LW, (13) Fujita SI-LC, (14) Fujita SI-LW-HC (99–1) composite, (15) Fujita SI-LW-HC (97.5–2.5), (16) Fujita SI-LW-HC (95–5), (17) Fujita SI-LW-HC (90–10), (D) PMF "Diesel", (G) PMF "Gasoline", (I) PMF "Regional/other". Profiles are discussed in Section 3.2.1 of the text. (a) Ratio–ratio plot for norhopane, hopane, and BC. (b) Ratio–ratio plot for trisnorhopane, hopane, and norhopane. (For interpretation of color in the figure legend, the reader is referred to the web version of the article.)

region defined by the PMF factor profiles that are not fit well by the PMF model. Fig. 6b shows a ratio–ratio plot of trisnorhopane and hopane normalized by norhopane. In this plot, the ambient data cluster to a point, which means that the ambient hopane data can be described by a single source profile. This plot suggests that the spread in the ambient data in Fig. 6a arises primarily from changes in BC emissions between sources of hopanes.

In Fig. 6a, the ambient norhopane-to-BC and hopane-to-BC ratios vary by over an order of magnitude. This variation could be due to changing emissions such as varying contributions of gasoline and diesel vehicles; it could also reflect changes in meteorology by mixing of emissions with different source profiles. However, the ambient data exhibit less variability than the published source profiles because each profile represents the emissions from a single or small number of sources while the ambient concentrations are a mixture of emissions from a large number of individual sources. The diesel source profiles cluster near the bottom left edge of the data, but the hopane-to-BC ratios of gasoline profiles vary widely. Low-emitting gasoline vehicles are enriched in BC relative to hopanes while high-emitting vehicles have low BC emissions.

One PMF factor ("diesel") describes 67% of the BC, 25% of the hopanes/steranes and about 50% of the C13–C18 *n*-alkanes. This factor exhibits strong diurnal and day-of-week patterns, as shown in Figs. 2d and 3d, which are consistent with mobile-source activity. Several pieces of evidence support association of this factor with diesel vehicle emissions. First, this factor falls within a cluster of diesel source profiles in the ratio-ratio plot shown in Fig. 6a. Second, the fractional apportionment of BC to this factor is consistent with previous work apportioning 67–94% of BC in Pittsburgh to diesel emissions (Subramanian et al., 2006). Finally, the field site was in close proximity to several major bus routes, which may be a potential source of high-emitting diesel vehicles.

A second factor "gasoline" contributed 20% of the BC, 45% of norhopane, 54% of hopane, and almost all of the VOCs included in the model. This factor is also distinguished by strong diurnal patterns consistent with mobile-source activity, as shown in Figs. 2d and 3d. From the factor composition, we believe this factor corresponds principally to gasoline vehicle activity. In Fig. 6a, this factor is located at the top right edge of the mixing line defined by the ambient data between the high- and low-emitter gasoline source profiles. In addition, this factor explains essentially all of the VOCs included in the model, which are thought to be predominantly emitted by gasoline-powered vehicles.

The third factor ("regional/other") contained 13% of the BC and high loadings for many of the PAHs, *n*-alkanes, 6,10,14-trimethyl-2-pentadecanone and 20% of the benzene. We cannot associate this factor with a specific source. A substantial fraction of hopanes/steranes are associated with this factor, indicating some contributions from a fossil fuel-based source or mixed contributions of multiple sources. The most likely explanation is that this "other" factor contains regional BC and organic markers, by virtue of no obvious diurnal/day-of-week patterns or source composition. The amount of BC apportioned to this factor (0.24 μg m^{-3}) is comparable with regional BC concentrations of 0.5 μg m^{-3} in the greater Pittsburgh area (Tang et al., 2004).

We investigated the sensitivity of the solution and the BC apportionment in particular by varying the amount of rotation ($-1.0 \leq$ FPEAK $\leq +1.0$), number of factors (3–5), and number of copies of BC (up to 5) included in the model. In every scenario, there is a BC-dominated factor with hopanes and a light aromatic VOC-dominated factor with a little bit of BC that presumably represent diesel and gasoline vehicles, respectively. Increasing the number of factors splits compounds primarily associated with the "regional" factor into multiple factors. Across the set of PMF models considered, the amount of BC apportioned to the "diesel" factor ranges from 67 to 100%, and BC apportioned to the "gasoline" and "regional" factors range from 0 to 20%. For the rotated solution (FPEAK $= -0.2$) discussed here, BC apportionment to the "diesel", "gasoline", and "regional/other" factors changed by up to 0.3%, 4.3%, and 11.5% with 5 copies of BC included in the model relative to the solution with a single copy of BC. The effects of rotations are discussed in detail in Supporting Information.

3.2.1. CMB analysis

CMB analysis was performed with BC and several hopanes (cholestane, trisnorhopane, norhopane, hopane, and homohopanes). 177 samples were analyzed using different combinations of source profiles. Each model included one composite diesel and one composite gasoline profile, selected based on the distribution of the ambient data relative to the source profiles shown in Fig. 6.

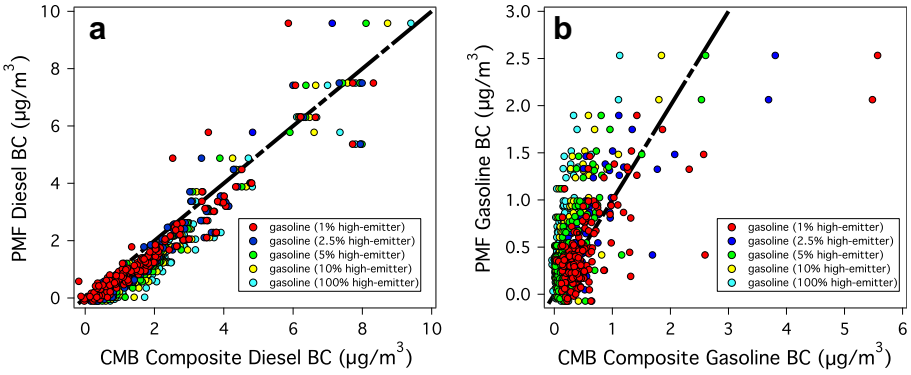

Fig. 7. Comparison of BC apportionment to PMF factors and CMB composite source profiles. (a) PMF "diesel" factor and CMB composite diesel profile over several CMB gasoline scenarios. (b) PMF "gasoline" factor and CMB composite gasoline profiles.

Diesel source profiles cluster at the bottom left corner of the ratio–ratio plot, meaning any diesel profile or combination of diesel profiles can be included in the model if it paired with a profile with a high hopane-to-BC ratio. Gasoline sources span the range of the ambient data in Fig. 6a, with low-emitters in the bottom left corner and high-emitters in the top right corner, so the composite gasoline vehicle fleet must contain enough high-emitters to describe the ambient data with large hopane-to-BC ratios. We considered a range of potential fleet compositions.

To assess the sensitivity of the CMB results to source profiles, we performed CMB analysis with multiple combinations of gasoline and diesel source profiles. CMB analysis was performed with three different diesel profiles: a medium-duty diesel profile (source #1 in Fig. 6, Fujita et al., 2007a), a heavy-duty diesel profile (source #3 in Fig. 6, Fujita et al., 2007a), and a 50:50 emission-weighted average composite of these two profiles (source #6 in Fig. 6). We also examined the effects of gasoline fleet composition on the CMB results by creating composite gasoline source profiles with different amounts of low- and high-emitting profiles shown in Fig. 6 (sources #12 and #6 or #8, Fujita et al., 2007a). We considered gasoline vehicle fleets of 1%, 2.5%, 5%, and 10% high-emitters on an emissions-weighted basis (sources #14–17). All CMB scenarios had acceptable statistical performance, with average $r^2 > 0.82$ and $\chi^2 < 1$.

Fig. 7 compares the BC apportioned to PMF mobile source factors to BC apportioned by CMB to source profiles. Fig. 7a shows results for diesel and Fig. 7b for gasoline. Results are plotted for different combinations of gasoline and diesel vehicle source profiles. There is excellent agreement between the BC apportioned to the PMF "diesel" factor and the CMB composite diesel profile ($m = 0.98$–1.02, $r^2 = 0.88$–0.94) regardless of the gasoline profile used. However, agreement in BC apportionment between the PMF "gasoline" factor and CMB composite gasoline profiles in Fig. 7b depends strongly on the gasoline source profile being used ($m = 0.44$–2.21, $r^2 = 0.50$–0.57 for 1–100% high-emitters). Overall, BC apportioned to gasoline vehicles with PMF and CMB agrees within a factor of 2 for most samples, with many data points clustered around the 1:1 line for the 1–5% high-emitter scenarios. The correlation in this regression analysis is worse than with the diesel apportionment.

Because diesel emissions are generally enriched in BC relative to gasoline emissions, and vice versa for hopanes, apportionment to gasoline vehicles is sensitive to how well CMB models hopane concentrations. Hopane levels in gasoline source profiles are highly variable relative to BC, and can vary by orders of magnitude depending on vehicle age, operating conditions, and other factors (Subramanian et al., 2006). In addition, the two highest concentration data points occurred during the event shown in Fig. 1d and strongly influence the parameters of the linear regression, as they are modeled very differently depending on the CMB scenario. These two points cause significant uncertainty in the regression for the profiles weighted by 1% and 2.5% high-emitters ($m = 0.44$ and $m = 0.65$), and may represent an isolated event not be due to motor vehicle emissions. Results indicate that the ambient fleet-average gasoline vehicle composition can be modeled by a composite profile containing somewhere between 1 and 5% high-emitters that contribute most of the emissions. The CMB model cannot differentiate within this range because of the variability in the hopane-to-BC ratios of the gasoline vehicle source profiles.

Using marker-to-OC and marker-to-$PM_{2.5}$-mass ratios of the source profiles, the CMB results also provide estimates of the gasoline and diesel OC and $PM_{2.5}$ concentrations. On a study-average basis, gasoline and diesel OC concentrations range from 0.25 to 1.3 and 1.2–2.0 μg C m^{-3} in downtown Pittsburgh, depending on the specific combination of source profiles. A number of other modeling studies have estimated gasoline and diesel vehicle contributions to fine particle concentrations in Pittsburgh. Previous CMB analyses of motor vehicle marker datasets from an urban background site in Pittsburgh also concluded diesel vehicles dominated the gas–diesel OC split (Subramanian et al., 2006; Bullock et al., 2008). We found stronger diesel dominance in this study, which is expected given the much higher BC levels downtown compared to the urban background site. Interestingly, an emission-based model implemented in PMCAMx determined gasoline vehicles dominated the gas–diesel OC split (Lane et al., 2007), which contrasts with results from receptor models.

Study-average gasoline and diesel $PM_{2.5}$ concentrations in downtown Pittsburgh ranged from 0.31 to 1.9 and 3.0–4.3 μg m^{-3}, or a gasoline–diesel $PM_{2.5}$ ratio of 0.09–0.56, indicating a diesel-dominated $PM_{2.5}$ split. This is also generally consistent with findings from other receptor- and emissions-based models for Pittsburgh (Subramanian et al., 2006; Lane et al., 2007; Bullock et al., 2008). However, relative gasoline contributions at the urban background site were higher: the gas–diesel $PM_{2.5}$ split approached 50–50% in some scenarios. The much stronger diesel dominance predicted downtown compared to the urban background is not surprising, as it is likely a consequence of proximity to more diesel vehicle activity. However, all of the receptor models predict a wide range of relative gas–diesel vehicle splits. Large variability in source profiles makes it impossible to constrain the relative split without significant uncertainty.

4. Conclusions

We have demonstrated the utility of high time-resolved molecular marker measurements with TAG for identifying sources

of organic aerosol. Emissions from mobile, point, and regional sources were identified based on different temporal and wind-direction patterns of organic molecular markers. Hopanes in downtown Pittsburgh appear to be contributed mostly by local motor vehicle emissions. Concentrations of other markers have strong wind-directional dependence that are consistent with known source activity, including PAHs from coke production. Oxidized markers like phthalic acid build up during the day but are relatively constant overall, indicating a regional source.

We compared results from PMF and CMB source apportionment, which is one of a few integrated PMF–CMB analyses of Pittsburgh molecular marker datasets (Shrivastava et al., 2007; Bullock et al., 2008). We also compared results with other emissions-based and receptor modes, and all calculations indicate diesel emissions are the dominant motor vehicle source, particularly in the downtown area. By including light aromatic VOCs in the PMF model, we were able to separate gasoline and diesel contributions. PMF analysis of the TAG data identified two factors that appear associated with mobile source emissions and a third BC factor that appears associated with regional emissions. Good agreement was observed between the PMF and CMB results for BC apportionment, and diesel vehicles dominated the gasoline–diesel OC and $PM_{2.5}$ splits in downtown Pittsburgh.

High time-resolved measurements played a crucial role in analysis of PMF factors through interpretation of factor time series data and average diurnal patterns. Mobile sources accounted for 87% of the BC, indicating their significant effect on air quality and potential exposure risk in downtown Pittsburgh. Recently-enacted idling restrictions in Allegheny County may help to significantly reduce diesel emissions, which contributed most of the $PM_{2.5}$ from mobile sources in this study.

Acknowledgements

We thank Brent Williams for contributions from previous work and helpful communication throughout this work. This work is supported by a grant from the Allegheny County Health Department and the U.S. Environmental Protection Agency. This paper has not been subject to EPA's required peer and policy review, and therefore does not necessarily reflect the views of the Agency. No official endorsement should be inferred.

Appendix. Supplementary information

Supplementary data associated with this article can be found, in the online version, at doi:10.1016/j.atmosenv.2009.04.057.

References

Allen, G.A., Lawrence, J., Koutrakis, P., 1999. Field validation of a semi-continuous method for aerosol black carbon (aethalometer) and temporal patterns of hourly black carbon measurements in southwestern PA. Atmos. Environ. 33 (5), 817–823.

Babich, P., Davey, M., Allen, G., Koutrakis, P., 2000. Method comparisons for particulate nitrate, elemental carbon, and PM2.5 mass in seven U.S. cities. J. Air Waste Manage. Assoc. 50, 1095–1105.

Bullock, K.R., Duvall, R.M., Norris, G.A., McDow, S.R., Hays, M.D., 2008. Evaluation of the CMB and PMF models using organic molecular markers in fine particulate matter collected during the Pittsburgh Air Quality Study. Atmos. Environ. 42, 6897–6904.

Coulter, C.T., December 2004. EPA-CMB8.2 Users Manual. http://www.epa.gov/scram001.

Falkovich, A., Rudich, Y., 2001. Analysis of semivolatile organic compounds in atmospheric aerosols by direct sample thermal desorption GC/MS. Environ. Sci. Technol. 35 (11), 2326–2333.

Friedlander, S.K., 1973. Chemical element balances and identification of air pollution sources. Environ. Sci. Technol. 7, 235–240.

Fujita, E.M., Campbell, D.E., Arnott, W.P., Chow, J.C., Zielinska, B., 2007a. Evaluations of the chemical mass balance method for determining contributions of gasoline and diesel exhaust to ambient carbonaceous aerosols. J. Air Waste Manage. Assoc. 57 (6), 721–740.

Fujita, E.M., Zielinska, B., Campbell, D.E., Arnott, W.P., Sagebiel, J.C., Mazzoleni, L., Chow, J.C., Gabele, P.A., Crews, W., Snow, R., Clark, N.N., Wayne, W.S., Lawson, D.R., 2007b. Variations in speciated emissions from spark-ignition and compression-ignition motor vehicles in California's South Coast Air Basin. J. Air Waste Manage. Assoc. 57 (6), 705–720.

Gold, M.D., Blum, A., Ames, B.N., 1978. Another flame retardant, tris-(1,3-dichloro-2-propyl)-phosphate, and its expected metabolites are mutagens. Science 200 (4343), 785–787.

Goldstein, A.H., Williams, B.J., Miller, A., Kreisberg, N.M., Hering, S.V., April 2008a. Hourly, in-situ quantitation of organic aerosol marker compounds, final report. California Air Resources Board Award No. 03-324. Tech. Rep.

Goldstein, A.H., Worton, D.R., Williams, B.J., Hering, S.V., Kreisberg, N.M., Panic, O., Gorecki, T., 2008b. Thermal desorption comprehensive two-dimensional gas chromatography for in-situ measurements of organic aerosols. J. Chromatogr. A 118, 340–347.

Hansen, A.D.A., Rosen, H., Novakov, T., 1984. The Aethalometer – an instrument for the real-time measurement of optical absorption by aerosol particles. Sci. Total Environ. 36, 191–196.

Ho, S.S.H., Yu, J.Z., Chow, J.C., Zielinska, B., Watson, J.G., Sit, E.H.L., Schauer, J.J., 2008. Evaluation of an in-injection port thermal desorption – gas chromatography/mass spectrometry method for analysis of non-polar organic compounds in ambient aerosol samples. J. Chromatogr. A 1200, 217–227.

Jaekels, J.M., Bae, M.-S., Schauer, J.J., 2007. Positive Matrix Factorization analysis of molecular marker measurements to quantify the sources of organic aerosols. Environ. Sci. Technol. 41, 5763–5769.

Jayne, J.T., Leard, D.C., Zhang, X., Davidovits, P., Smith, K.A., Kolb, C.E., Worsnop, D.R., 2000. Development of an Aerosol Mass Spectrometer for size and composition analysis of submicron particles. Aerosol Sci. Technol. 33, 49–70.

Kreisberg, N.M., Hering, S.V., Williams, B.J., Worton, D.R., Goldstein, A.H., 2009. Quantification of hourly speciated organic compounds in atmospheric aerosols, measured by an in-situ Thermal Desorption Aerosol Gas Chromatograph (TAG). Aerosol Sci. Technol. 43 (1), 38–52.

Lane, T.E., Pinder, R.W., Shrivastava, M.K., Robinson, A.L., Pandis, S.N., 2007. Source contributions to primary organic aerosol: comparison of the results of a source-resolved model and the chemical mass balance approach. Atmos. Environ. 41, 3758–3776.

Lavrich, R.J., Hays, M.D., 2007. Validation studies of Thermal Extraction-GC/MS applied to source emissions aerosols. 1. Semivolatile analyte-nonvolatile matrix interactions. Anal. Chem. 79 (10), 3635–3645.

Legreid, G., Reimann, S., Steinbacher, M., Staehelin, J., Young, D., Stemmler, K., 2007. Measurements of OVOCs and NMHCs in a Swiss highway tunnel for estimation of road transport emissions. Environ. Sci. Technol. 41 (20), 7060–7066.

Logue, J.M., Hartz, K.E.H., Lambe, A.T., Donahue, N.M., Robinson, A.L. High time resolved measurements of organic air toxics in multiple exposure regimes. Atmos. Environ. (submitted for publication).

Norris, G., Vedantham, R., Wade, K., Brown, S., Prouty, J., Foley, C., July 2008. EPA Positive Matrix Factorization (PMF) 3.0 Fundamentals and User Guide.

Ondov, J.M., Buckley, T.J., Hopke, P.K., Ogulei, D., Parlange, M.B., Rogge, W.F., Squibb, K.S., Johnston, M.V., Wexler, A.S., 2006. Baltimore Supersite: highly time- and size-resolved concentrations of urban PM2.5 and its constituents for resolution of sources and immune responses. Atmos. Environ. 40, S224–S237.

Paatero, P., 1999. The multilinear engine – a table-driven, least squares program for solving multilinear problems, including the n-way parallel factor analysis model. J. Comput. Graphical Stat. 8, 854–888.

Paatero, P., Hopke, P.K., Begum, B.A., Biswas, S.K., 2005. A graphical diagnostic method for assessing the rotation in factor analytical models of atmospheric pollution. Atmos. Environ. 39 (1), 193–201.

Paatero, P., Tapper, U., 1994. Positive Matrix Factorization: A non-negative factor model with optimal utilization of error estimates of data values. Environmetrics 5, 111–126.

Park, S.S., Kim, Y.J., Fung, K., 2002. PM2.5 carbon measurements in two urban areas: Seoul and Kwanju, Korea. Atmos. Environ. 36 (8), 1287–1297.

Riddle, S.G., Robert, M.A., Jakober, C.A., Hennigan, M.P., Kleeman, M.J., 2007. Size distribution of trace organic species emitted from light-duty vehicles. Environ. Sci. Technol. 41 (21), 7464–7471.

Robinson, A.L., Donahue, N.M., Rogge, W.F., 2006a. Photochemical oxidation and changes in molecular composition of organic aerosol in the regional context. J. Geophys. Res. 111, D3302. doi:10.1029/2005JD006265.

Robinson, A.L., Subramanian, R., Bernando-Bricker, A., Rogge, W.F., 2006b. Source apportionment of molecular markers and organic aerosol. 2. Biomass smoke. Environ. Sci. Technol. 40, 7811–7819.

Robinson, A.L., Subramanian, R., Donahue, N.M., Bernando-Bricker, A., Rogge, W.F., 2006c. Source apportionment of molecular markers and organic aerosol. 1. Polycyclic aromatic hydrocarbons and methodology for data visualization. Environ. Sci. Technol. 40, 7803–7810.

Rogge, W.F., Hildemann, L.M., Mazurek, M.A., Cass, G.R., 1996. Mathematical modeling of atmospheric fine particle-associated primary organic compound concentrations. J. Geophys. Res. 101 (D14), 19379–19394.

Rogge, W.F., Hildemann, L.M., Mazurek, M.A., Cass, G.R., Simoneit, B.R.T., 1993a. Sources of fine organic aerosol. 2. Noncatalyst and catalyst-equipped automobiles and heavy-duty diesel trucks. Environ. Sci. Technol. 27, 636–651.

Rogge, W.F., Hildemann, L.M., Mazurek, M.A., Cass, G.R., Simoneit, B.R.T., 1993b. Sources of fine organic aerosol. 5. Natural gas home appliances. Environ. Sci. Technol. 27, 2736–2744.

Rogge, W.F., Hildemann, L.M., Mazurek, M.A., Cass, G.R., Simoneit, B.R.T., 1997. Sources of fine organic aerosol. 8. Boilers burning No. 2 distillate fuel oil. Environ. Sci. Technol. 31, 2731–2737.

Schauer, J.J., Cass, G.R., 2000. Source apportionment of wintertime gas-phase and particle-phase air pollutants using organic compounds as tracers. Environ. Sci. Technol. 34, 1821–1832.

Schauer, J.J., Fraser, M.P., Cass, G.R., Simoneit, B.R.T., 2002a. Source reconciliation of atmospheric gas-phase and particle-phase pollutants during a severe photochemical smog episode. Environ. Sci. Technol. 36, 3806–3814.

Schauer, J.J., Kleeman, M.J., Cass, G.R., Simoneit, B.R.T., 2002b. Measurement of emissions from air pollution sources. 5. C1–C32 organic compounds from gasoline-powered motor vehicles. Environ. Sci. Technol. 36, 1169–1180.

Schauer, J.J., Kleeman, M.J., Cass, G.R., Simoneit, B.R.T., 1999. Measurement of emissions from air pollution sources. 2. C1 through C30 organic compounds from medium duty diesel trucks. Environ. Sci. Technol. 33, 1578–1587.

Schauer, J.J., Rogge, W.F., Hildemann, L.M., Mazurek, M.A., Cass, G.R., 1996. Source apportionment of airborne particulate matter using organic compounds as tracers. Atmos. Environ. 30 (22), 3837–3855.

Schmid, H., Pucher, E., Ellinger, R., Biebl, P., Puxbaum, H., 2001. Decadal reductions of traffic emissions on a transit route in Austria – results of the Tauerntunnel experiment 1997. Atmos. Environ. 35 (21), 3585–3593.

Shrivastava, M.K., Subramanian, R., Rogge, W.F., Robinson, A.L., 2007. Sources of organic aerosol: positive matrix factorization of molecular marker data and comparison of results from different source apportionment models. Atmos. Environ. 41, 9353–9369.

Simoneit, B.R.T., Medeiros, P.M., Didyk, B.M., 2005. Combustion products of plastics as indicators for refuse burning in the atmosphere. Environ. Sci. Technol. 39, 6961–6970.

Solomon, P.A., Sioutas, C., 2008. Continuous and semicontinuous monitoring techniques for particulate matter mass and chemical components: a synthesis of findings from EPA's Particulate Matter Supersites program and related studies. J. Air Waste Manage. Assoc. 58 (2), 164–195.

Stolzenburg, M.R., Hering, S.V., 2000. A new method for the automated measurement of atmospheric fine particle nitrate. Environ. Sci. Technol. 34, 907–914.

Subramanian, R., Donahue, N.M., Bernando-Bricker, A., Rogge, W.F., Robinson, A.L., 2006. Contribution of motor vehicle emissions to organic carbon and fine particle mass in Pittsburgh, Pennsylvania: effects of varying source profiles and seasonal trends in ambient marker concentrations. Atmos. Environ. 40, 8002–8019.

Takegawa, N., Miyakawa, T., Kawamura, K., Kondo, Y., 2007. Contribution of selected dicarboxylic and w-oxocarboxylic acids in ambient aerosol to the m/z 44 signal of an Aerodyne Aerosol Mass Spectrometer. Aerosol Sci. Technol. 41 (4), 418–437.

Tang, W., Raymond, T., Witting, B., Davidson, C.I., Pandis, S.N., Robinson, A.L., Crist, K., 2004. Spatial variations of $PM_{2.5}$ during the Pittsburgh Air Quality Study. Aerosol Sci. Technol. 38, 80–90.

Thoma, E.D., Shores, R.S., Isakov, V., Baldauf, R.W., 2008. Characterization of near-road pollutant gradients using path-integrated optical remote sensing. J. Air Waste Manage. Assoc. 58, 879–890.

Waterman, D., Horsfield, B., Hall, K., Smith, S., 2001. Application of micro-scale sealed vessel thermal desorption–gas chromatography–mass spectrometry for the organic analysis of airborne particulate matter: linearity, reproducibility, and quantification. J. Chromatogr. A. 912, 143–150.

Weitkamp, E.A., Lambe, A.T., Donahue, N.M., Robinson, A.L., 2008. Laboratory measurements of the heterogeneous oxidation of condensed-phase organic molecular markers for motor vehicle exhaust. Environ. Sci. Technol. 42 (21), 7950–7956.

Wexler, A.S., Johnston, M.V., 2008. What have we learned from highly time-resolved measurements during EPA's Supersites program and related studies? J. Air Waste Manage. Assoc. 58 (2), 303–319.

Williams, B.J., Goldstein, A.H., Kreisberg, N.M., Hering, S.V., 2006. An in-situ instrument for speciated organic composition of atmospheric aerosols: Thermal Desorption Aerosol GC/MS-FID (TAG). Aerosol Sci. Technol. 40, 627–638. doi:10.1080/02786820600754631.

Williams, B.J., Goldstein, A.H., Millet, D.B., Holzinger, R., Kreisberg, N.M., Hering, S.V., White, A.B., Worsnop, D.R., Allan, J.D., Jimenez, J.L., 2007. Chemical speciation of organic aerosol during the International Consortium for Atmospheric Research on Transport and Transformation 2004: results from in situ measurements. J. Geophys. Res. 112, D10S26.

Zheng, M., Cass, G.R., Schauer, J.J., Edgerton, E.S., 2002. Source apportionment of PM2.5 in the southeastern United States using solvent-extractable organic compounds as tracers. Environ. Sci. Technol. 36, 2361–2371.